Published in final edited form as:
Cell Immunol. 2009 ; 254(2): 124–134. doi:10.1016/j.cellimm.2008.08.003.

129/SvJ mice have mutated CD23 and hyper IgE

Jill W. Ford[1,*], **Jamie L. Sturgill**[1], and **Daniel H. Conrad**[1,**]
1*Virginia Commonwealth University*

Abstract

CD23, the low affinity IgE receptor, is hypothesized to function as a negative regulator of IgE production. Upon discovering reduced CD23 surface levels in 129/SvJ inbred mice, we sought to further investigate 129/SvJ CD23 and to examine its influence on IgE levels. Five amino acid substitutions were found in 129/SvJ CD23. Identical mutations were also observed in CD23 from New Zealand Black and 129P1/ReJ mice. 129/SvJ B cells proliferated more rapidly than those from BALB/c after stimulation with IL-4 and CD40 ligand trimer. However, *in vitro* IgE levels in supernatants from stimulated 129/SvJ B cells were significantly reduced. Contrary to the *in vitro* findings, the 129/SvJ CD23 mutations correlated with a hyper IgE phenotype *in vivo* and 129/SvJ were able to clear *Nippostrongylus brasiliensis* infection more rapidly than either BALB/c or C57BL/6. Overall, this study further suggests that CD23 is an important regulatory factor for IgE production.

Keywords

129/SvJ mouse; B cells; CD23; Hyper IgE; Helminth

Introduction

The low affinity IgE receptor, CD23 (FcεRII), is a type II transmembrane protein and a member of the calcium-dependent (C-type) lectin family [1]. In the mouse system, CD23 is expressed on the B lymphocyte, the follicular dendritic cell and the gut epithelium [2] whereas in the human system, CD23 can be found on B cells, monocytes, eosinophils, and Langerhans cells. CD23 consists of four domains, including a carboxy-terminal lectin head, a stalk region, a transmembrane domain, and a short, cytoplasmic tail. Based on molecular modeling studies, Gould and colleagues proposed a model whereby CD23 oligomerizes, with two of the lectin heads of the trimer binding to one IgE molecule, resulting in a high avidity interaction of CD23 with IgE [3]. CD23 contains two cleavage sites within its stalk domain and is cleaved from the cell surface by the metalloprotease ADAM10,[4] resulting in soluble CD23 (sCD23) fragments [5;6]. sCD23 consists primarily of the lectin domain, with varying amounts of stalk, and is thus capable of binding to IgE, albeit with a lower avidity than that of oligomeric CD23 [6;7].

Since its discovery, CD23 has been proposed to play a role in regulating IgE levels. The finding that IL-4 increased both the expression of IgE as well as that of CD23 led to the hypothesis that CD23 could serve as a natural means to dampen IgE responses. Recently, CD23's role as

**Please send correspondence to Daniel H. Conrad, Department of Microbiology and Immunology, Virginia Commonwealth University, PO Box 980678, MCV Station, Richmond, VA 23298. Fax: 804-828-9946. Phone: 804-828-2311. E-mail: dconrad@vcu.edu.
*Current address: Laboratory of Experimental Immunology, NCI-Frederick

a negative regulator of IgE production *in vivo* has been demonstrated through studies utilizing CD23 transgenic and CD23 knockout mice as well as antibodies targeting CD23. CD23 deficient mice, on a C57BL/6 background, produce higher amounts of IgE than littermate controls after stimulation with Ag-alum [8] while mice overexpressing CD23, regardless of background strain make significantly less IgE in response to the same stimuli [9;10]. Injection of mice with a polyclonal rabbit anti-stalk CD23 results in increased serum IgE levels [11]. We have recently shown that destabilization of CD23 via injection of a rat anti-stalk CD23 (19G5) enhanced the cleavage of CD23 from the cell surface and increased serum IgE levels [12]. Collectively, these data demonstrate that CD23 is an important control factor for IgE production *in vivo*.

129/SvJ mice are frequently used for gene targeting studies due to the availability of several embryonic stem cell lines that have been derived from them (reviewed in [13]). Over the past 10 years, several immunological defects have been uncovered in the 129 strains, thus questioning their usefulness in gene targeting studies without sufficient backcrossing. Corcoran and Metcalf [14] observed that B cells from 129/Sv and 129/Ola mice were defective in signaling downstream of the IL-5 receptor, which could be explained at least in part by reduced expression of the IL-5R alpha chain. McVicar *et al* [15] found that natural killer cells were defective in their ability to signal through the receptor DAP12. Recently, Kaminski and Stavnezer [16] showed that 129/Sv spleens had more marginal zone B cells compared with those from C57BL/6 mice. In addition, they observed that 129/Sv B cells were defective in their class switching to IgG3 *in vitro*. 129/Sv mice have also recently been reported to have defects in their mast cell signaling downstream of the FcεRI. Yamashita *et al* [17] found that 129/Sv mice had greater expression levels of FcεRI and that ligation of the FcεRI resulted in increased mast cell degranulation. They also noted that the 129/Sv mice had increased anaphylaxis as compared to C57BL/6 mice.

In this study we demonstrate that CD23 is mutated in 129/SvJ mice. This mutated CD23 is associated with reduced CD23 surface levels and increased serum IgE production in the 129/SvJ strain as compared to the BALB/cJ strain. Overall, the data lend further support to CD23's role as a negative regulator of IgE production and demonstrate that the 129/SvJ strain may be beneficial for the study of allergic diseases.

Materials and Methods

Animals

BALB/c and C57BL/6 mice were purchased from the National Cancer Institute (Frederick, MD). BALB/cJ, C57BL/6J, 129/SvJ, 129P1/ReJ, and NZB mice were purchased from the Jackson Laboratory (Bar Harbor, ME). CD23 deficient mice [18] were generated as described and maintained at VCU. All mice used were between 6-16 weeks of age at the start of the experiment and were housed in an accredited and pathogen-free animal facility. Female mice were primarily used. All studies were approved by the VCU IACUC.

Preparation and purification of monoclonal antibodies

The monoclonal antibodies 19G5, 2H10, B3B4, B1E3, R1E4, 2.4G2, and mouse IgE anti-DNP were prepared from cell culture supernatants using CL-1000 Adhere CELLine flasks (Integra Biosciences, Switzerland). Cells were grown in complete RPMI (RPMI 1640 supplemented with 10% heat inactivated FBS, 100 U/ml penicillin and streptomycin, 2mM L-glutamine, 10mM HEPES, and 5×10^{-5} M 2-mercaptoethanol) supplemented with 2 μg/ml gentamicin. Supernatants harvested from CELLine flasks were centrifuged at 2000 RPM for 5 minutes, filtered through a 0.8 micron filter (PALL Life Sciences, Ann Arbor, MI), and stored at -20° C until purification. Just prior to purification, cell supernatants were further clarified by

centrifugation at 20,000 × g for 30 minutes. Antibody purification was performed by hydrophobic charge induction chromatography using MEP HyperCel sorbent (PALL Life Sciences, East Hills, NY) [19].

B cell purification and culture

B cells were purified from spleens by negative selection as previously described [20]. Briefly, T cells in single cell suspensions were coated with antibodies and depleted by complement lysis. The remaining spleen cells were layered over a discontinuous Percoll (GE Healthcare) gradient [21]. Resting B cells selected from the 66-70% interface were used for *in vitro* proliferation studies and Ig analyses. For some experiments (*i.e*. RNA isolation and Scatchard analysis), total B cells (50-70% Percoll interface) were used. B cells were cultured in B cell media consisting of RPMI 1640 supplemented with 10% heat inactivated FBS, 100 U/ml penicillin and streptomycin, 2mM L-glutamine, 1mM sodium pyruvate, 10mM HEPES, 100mM non-essential amino acids and 5×10^{-5} M 2-mercaptoethanol.

To examine IgE, IgG1, and IgM production, resting B cells were cultured in 96 well plates (Corning Life Sciences, Lowell, MA) at varying concentrations (50,000 – 250 cells/well) in 200 μl B cell media containing 10,000 U/ml recombinant mouse IL-4 (kindly provided by William Paul), 5 ng/ml mouse IL-5 (eBioscience, San Diego, CA), 25 ng/ml mouse CD40LT, and 100 ng/ml M15 (anti-leucine zipper). Both CD40LT and M15 [22] were generous gifts from Amgen, Seattle, WA. For IL-4 dose response studies, 5000 cells per well were stimulated as above with IL-5, CD40LT, and M15 in the presence of increasing concentrations of IL-4. Supernatants were harvested after 8 days of culture and analyzed by ELISA.

For proliferation studies, purified resting B cells were cultured as above and were pulsed with 1 μCi per well ^{3}H-thymidine (MP Biomedicals, Irvine, CA) during the last eight hours of a 72 hour incubation. Plates were harvested using a Filtermate 196 harvester onto a Unifilter 96 well plate. 30 μl of Microscint-20 scintillation fluid was added to each well and plates were counted using a Top Count Scintillation Microplate Reader. Harvester, scintillation fluid, and counter were all from Perkin Elmer (Boston, MA). Alternatively, purified B cells were labeled with carboxyfluorescein succinimidyl ester (CFSE) as described [23]. Labeled cells were cultured as above and on indicated days, the amount of CFSE labeling remaining was determined by FACS analysis.

For stimulation of B cells for RNA isolation, flow cytometry, and Scatchard analyses, purified total B cells were incubated in 24 well plates (Greiner Bio-One North America, Monroe, NC) containing 1 ml of B cell media supplemented with 10,000 U/ml recombinant mouse IL-4, 25 ng/ml mouse CD40LT, and 100 ng/ml M15. Cells were harvested at either 24 or 48 hours depending on the assay.

RNA isolation and analysis

Total RNA was isolated from unstimulated total B cells or IL-4 and CD40LT activated total B cells using Trizol reagent as recommended by the manufacturer (Invitrogen). For quantitative PCR analysis (qPCR), the use of the TaqMan® One Step PCR Master Mix Reagent Kit was employed. All the samples were tested in triplicate under the conditions recommended by the fabricant. The cycling conditions were: 48C/30min; 95C/10min; and 40 cycles of 95C/15sec and 60C/1min. The cycle threshold was determined to provide the optimal standard curve values (.98 to 1.0). The experiments were performed in the ABI Prism® 7900 Sequence Detection System (Applied Biosystems, Foster City, Ca) The probes and primers were designed using the Primer Express® 2.0 version. The probes were labeled in the 5' end with FAM (6-carboxyfluoresceine) and in the 3' end with TAMRA (6-carboxytetramethylrhodamine). Ribosomal RNA (18S rRNA) from the Pre-developed TaqMan®Assay Reagents was used as

endogenous control. The reactions and the synthesis of the probes and primers were performed in the VCU Nucleic Acid Research Facilities.

For RT-PCR analysis, reactions were performed using the EPICENTRE MasterAmp High Fidelity RT-PCR Kit (EPICENTRE, Madison, WI) according to the manufacturer's protocol. Briefly, total RNA (1000 ng/reaction) was mixed with mouse CD23 specific primers (12.5 pmoles/reaction) and sterile nuclease-free water in a reaction mix containing 1X MasterAmp RT-PCR PreMix, 40 Units MMLV-RT (Moloney Murine Leukemia Virus Reverse Transcriptase) Plus, and 1 Unit MasterAmp TAQurate DNA Polymerase Mix to a final volume of 50 μl. The forward (CTGCCATGGAAGAAAATG) and reverse (TGAGCAGAAGTTTGTCAGG) primers were designed to amplify the entire coding sequence of CD23. Reactions were also set up using primers specific for mouse actin [24] as an internal control. The following cycle was used: 65°C for 5 min, 37°C for 30 min, 95°C for 1 min, 95°C for 30 sec, 45°C for 30 sec, 70°C for 1 min 10 sec, 72°C for 7 min.

Cloning and sequence analysis

Purified total B cells isolated from the spleens of 129/SvJ, 129P1/ReJ, and NZB mice were stimulated for 48 hours at 1×10^6 cells per well in 1 ml B cell media containing IL-4, CD40LT, and M15. RNA was isolated and RT-PCR was carried out as described above using murine CD23 sense and murine CD23 antisense primers. The 1.1 Kb PCR product was inserted into pCR2.1 (Invitrogen) and positive colonies were identified by *Eco*RI digest. Sequencing was performed by the VCU Nucleic Acids Core Facility using the ABI 3100 capillary sequencer. Sequencing of both strands, using the T7 and M13R primers was done on 4 separate clones from 129SvJ, 129P1/SvJ and 3 clones of NZB and the values compared, the sequences shown were identical for the 129 and NZB CD23 containing clones. Balb CD23 sequence is accession #NP_038545. Sequence analysis was performed using Vector NTI software (Invitrogen) using the ContigExpress and alignment programs.

FACS analysis

1×10^6 cells per tube were incubated with 10 μg 2.4G2 in 200 μl FACS buffer (1X PBS, 1% FBS) for 15 minutes at 4°C to block the FcγR and then stained with FITC-B3B4 (anti-lectin CD23) and APC-B220 (anti-CD45R) for 1 hour at 4°C in the dark. Alternatively, cells were incubated with biotinylated rabbit anti-LZ-CD23 or biotinylated 2H10 (anti-lectin CD23) for 30 minutes, washed, resuspended in 200 μl FACS buffer, and then stained with goat-anti-biotin-FITC and APC-B220 for 1 hour. To test IgE binding to B cells, splenocytes were incubated with 20 μg mouse IgE-anti-DNP for 30 minutes, washed, resuspended in 200 μl FACS buffer, and then stained with FITC-anti-mouse IgE and APC-B220 for 1 hour. After staining, cells were washed once with 1X PBS and resuspended in 1 ml of FACS buffer. Flow cytometric analysis was performed using the FC500 combined with CXP software (Beckman Coulter, Fullerton, CA).

Scatchard analysis

Mouse IgE was labeled with [^{125}I]-NaI (Perkin Elmer) using the Chloramine T method as previously described [25]. Purified total B cells from 129/SvJ or BALB/c mice were stimulated in 24 well plates for 48 hours at a concentration of 1×10^6 cells per ml in 1 ml B cell media containing IL-4, CD40LT, and M15. Cells were harvested and counted. 1×10^6 cells were added to tubes containing Binding Assay Buffer [BAB (Hank's Balanced Salt Solution, 2% FBS, 10mM HEPES, 1mM $CaCl_2$)] and 10 μg 2.4G2 and were allowed to equilibrate to 37°C in a water bath. 0.5 or 5.0 μg ^{125}I-labeled IgE was added to the cells in the presence of increasing concentrations of cold IgE (1.0 - 400ug/ml) to a final volume of 300 μl BAB per tube. The cells were incubated with the hot and cold IgE for 1 hour at 37°C. Duplicate aliquots were removed and layered over phthalate oil as previously described [26]. Free and cell-

bound ^{125}I-IgE was separated by centrifugation over the phthalate oil mixture. Cell pellet radioactivity was read using the LKB Clinigamma 1272 gamma counter (Perkin Elmer). Non-specific binding was determined by adding ^{125}I-IgE to purified CD23 deficient B cells and this value was subtracted to obtain specific binding. Scatchard plots of the data allowed binding affinities to be determined by linear regression analysis. The number of binding sites per cell was calculated by extrapolating to the x-axis and all lines had correlation coefficients of 0.75 or better.

Immunizations and bleeds

BALB/cJ and 129/SvJ mice were pre-bled by tail vein nick and injected s.c. on day 0 with 100μg KLH-DNP and 4mg alum in 200 μl PBS. Control groups received alum only. Mice were bled on day 9, boosted on day 15, and bled on day 20. Serum was analyzed for Ig levels by ELISA.

Nippostrongylus brasiliensis isolation and culture

Nb was kindly provided by Dr. Joseph Urban, Jr. (USDA, Beltsville, MD) and was maintained by passage through BALB/c mice. *Nb* was isolated from fecal cultures using the Baermann Technique as previously described [27]. BALB/cJ or 129/SvJ mice were pre-bled and injected s.c. on day 0 with 650 L3 larvae in 100 μl NaCl. Mice were bled on days 9, 15, 23, and 43 and serum was assayed for IgE levels by ELISA. To examine parasite clearance, BALB/c, C57BL/6, or 129/SvJ mice were injected with 650 L3 larvae. Three mice per strain were sacrificed on days 5-9. Small intestines were removed and examined for L5 *Nb* as described [27]. Briefly, longitudinal slices in the intestines were made using dissecting scissors. The sliced intestines were placed over an 8 × 8 cm square of cheese cloth (Prym-Dritz Corporation, Spartanburg, SC) and dipped into a 50 ml tube containing PBS such that the intestines were submerged but the corners of the cheese cloth were trapped beneath the tube cap. The tubes were incubated in a 37°C water bath for 2 hours to allow complete migration of the worms out of the intestines and into the PBS. The worms collected at the bottom of the tube were counted by dividing them among the wells of a 48 well plate (Greiner Bio-One).

ELISAs

IgE levels in mouse serum were determined by coating Immulon ELISA plates with 10 μg/ml of the rat anti-mouse IgE mAb B1E3. Standard curves were generated with mouse IgE anti-DNP. IgE levels were detected by incubation with the biotinylated rat anti-mouse IgE mAb R1E4 followed by streptavidin-AP. Plates were developed using pNPP substrate tablets and read at a dual wavelength of 405-650 nm. Plates were read with a Spectromax 250 ELISA plate reader (Molecular Devices, Sunnyvale, CA). A four parameter analysis was performed on standard curves using Molecular Devices software and correlation coefficients were >.98 or better. Only dilution values that fell in the linear portion of the curve were used for analysis and experimental values at multiple dilutions were averaged.

IgG1 and IgM levels were determined similarly by coating plates with 5 μg/ml unlabeled goat anti-mouse IgG1 or goat anti-mouse IgM and detecting with goat-anti-mouse IgG1-AP or goat-anti-mouse IgM-AP, respectively. Standard curves were generated with mouse IgG1 or mouse IgM.

For detection of KLH-DNP-specific IgE, plates were coated with 10 μg/ml B1E3. Standard curves were generated as above with the total IgE ELISA. KLH-DNP-specific IgE was detected using biotinylated KLH-DNP followed by Strep-AP. For detection of KLH-DNP-specific IgG1, plates were coated with 10 μg/ml KLH-DNP for sample wells and 5 μg/ml unlabeled goat anti-mouse IgG1 for standard wells. KLH-DNP-specific IgG1 was detected using goat-anti-mouse-IgG1-AP as above.

To detect sCD23 levels, plates were coated with 20 μg/ml of the rabbit polyclonal mouse anti-LZ-CD23. Serum samples and standards (EC-CD23) were detected using biotinylated rabbit polyclonal mouse anti-CD23 followed by goat anti-biotin-HRP.

Statistics

Where shown, *P* values were determined using unpaired Student's *t* test.

Results

CD23 surface expression is reduced on 129/SvJ B cells

To measure B cell CD23 levels, splenocytes from BALB/c or 129/SvJ mice were stained using B3B4, a mAb recognizing the lectin domain of CD23, and analyzed by flow cytometry. Less CD23 was observed on B cells from 129/SvJ mice as compared to those from BALB/c mice (MFI of 4.2 vs 6.8) (Fig.1A). A polyclonal anti-CD23 was used to confirm the reduced levels observed in the 129/SvJ mouse. Although expression was slightly enhanced using the polyclonal Ab, CD23 levels on the 129/SvJ B cells remained lower than those on the BALB/c B cells (data not shown). To determine if 129/SvJ CD23 levels could be upregulated, we isolated B cells from the spleens of 129/SvJ or BALB/c mice, stimulated them for 48 hours with IL-4 and CD40LT, and analyzed surface expression by flow cytometry using B3B4. Although 129/SvJ CD23 expression was increased after stimulation, levels were still lower than those observed on stimulated BALB/c B cells (MFI of 74 vs 276) (Fig. 1B). The MFI changes show that the fold increase in CD23 is higher in Balb/c (17.8 vs 41.3-fold) going from $CD23^+$ naïve B to stimulated $CD23^+$ B cells.

No significant difference in CD23 mRNA expression in 129/SvJ versus BALB/c B cells

To determine if 129/SvJ CD23 was regulated at the transcriptional level, we analyzed CD23 message levels in unstimulated and IL-4 and CD40LT activated B cells initially by RT-PCR (data not shown), with a confirmation using real time PCR (qPCR). CD23 message levels in both 129/SvJ and BALB/c B cells were similar before stimulation. After activation with IL-4 and CD40LT, CD23 mRNA levels in B cells from both strains were increased to a similar extent (Fig 2) with no significant difference noted between strains.

129/SvJ serum sCD23 levels are reduced

The reduced cell surface CD23 levels observed in the 129/SvJ B cells could be the result of decreased translation, decreased transport to the cell surface, or increased shedding of CD23 from the cell membrane. To address the possibility that the reduced CD23 expression seen in the 129/SvJ B cells was due to increased shedding of 129/SvJ CD23 from the cell surface, we injected 129/SvJ and C57BL/6 mice with the anti-CD23 stalk monoclonal 19G5 to induce shedding or PBS as a vehicle control. Three days later, mice were bled and sCD23 was measured by ELISA. Whereas the serum sCD23 levels in the PBS injected C57BL/6 and 129/SvJ mice measured 7.9±3.2 and 5.9±0.3 ng/ml, respectively, the sCD23 levels in the 19G5 injected C57BL/6 and 129/SvJ mice increased to 1127±56.7 and 627±52.5 ng/ml, respectively. Although the anti-CD23 injection enhanced sCD23 levels in both strains, the average levels of sCD23 in the 19G5-injected 129/SvJ mice were significantly lower than those in the 19G5-injected C57BL/6 mice ($P>.05$). Since cell surface levels were reduced, this change could be expected.

129/SvJ CD23 is mutated

The reduced levels of CD23 surface expression in the 129/SvJ mice led us to examine the 129/SvJ CD23 sequence. B cells isolated from the spleens of 129/SvJ mice were stimulated for 48 hours with IL-4 and CD40LT. RNA was isolated and CD23 cDNA was amplified by RT-PCR.

Sequence comparison to BALB/c is shown in Fig 3A. Compared to BALB/c, the CD23 sequence in 129/SvJ contained 5 mutations; three in the stalk region (A82T, V87A, and K131E) and two within the lectin domain (S258L and D301N) (Fig. 3A). A diagram indicating the location of these mutations within the CD23 protein is shown in Fig. 3B. The examination of published sequences of CD23 from other strains revealed that 4 out of the 5 a.a. mutations in the 129/SvJ strain were identical to those recently reported in the NZB mouse while the CD23 sequences in the BALB/c, C57BL/6, and DBA strains were 100% conserved at the amino acid level [28]. To determine if the CD23 mutations were unique to the 129/SvJ and NZB strains or if they were shared by other 129 strains, we sequenced CD23 from the 129P1/ReJ. Additionally, we sequenced CD23 from the NZB mouse to determine if the fifth mutation that we observed in the 129/SvJ strain (the one not previously reported by Lewis *et al*) was also present. The CD23 sequences in both the 129P1/ReJ and the NZB mice were identical to that found in the 129/SvJ strain (Fig.3A). Based on the genealogy of the 129 strains [29], it is likely that all the 129 substrains will have these 5 mutations within their CD23 gene.

129/SvJ B cells have a reduced number of IgE binding sites but a similar affinity for IgE

Reduced CD23 levels in 129/SvJ mice should correspond to fewer IgE binding sites. Because we predicted that the 129/SvJ CD23 mutations would impair the ability of CD23 to associate into trimers, we hypothesized that 129/SvJ CD23 may bind IgE with a lower affinity than BALB/c CD23. Saturation binding assays using labeled mouse IgE confirmed that there were fewer IgE binding sites on the 129/SvJ B cells than on the BALB/c B cells (Table I). In general, the 129 B cell preparations had a slightly higher level of CD23 negative cells. As a result, the difference in CD23 levels per positive B cell is less than indicated in Table I. However, Scatchard analysis revealed that the affinity constants of BALB/c CD23 and 129/SvJ CD23 for IgE were similar (Table I).

129/SvJ B cells have defective Ig production in vitro

Because 129/SvJ B cells have mutated CD23 and reduced CD23 levels, we hypothesized that they would produce more IgE upon stimulation with IL-4 and CD40LT. To investigate this hypothesis, we isolated B cells from the spleens of BALB/c and 129/SvJ mice and stimulated them in the presence of IL-4, IL-5, and CD40LT. After 3 and 8 days, we assessed B cell proliferation by measuring ^{3}H-thymidine incorporation and IgM production by ELISA, respectively. 129/SvJ B cells proliferated more rapidly than BALB/c B cells (Fig.4A) in response to IL-4, IL-5 and CD40LT. In view of this finding, we examined cell division of CFSE labeled cells at 24 hr intervals. Cells were stimulated as in the ^{3}H-thymidine experiment. While more rapid cell division in 129 B cells was evident at 48 hrs (Fig 4B), by 3 days (72 hrs), the Balb/c and 129 B cells had similar numbers of cell divisions (Fig 4C), thus indicating that the enhancement of proliferation in the 129 B cells was transient.

In the 8 day cultures, IgM levels in supernatants from 129/SvJ stimulated B cells were elevated versus those observed in BALB/c B cell cultures (Fig.5A). However, IgE levels in the supernatants of 129/SvJ B cells activated with IL-4, IL-5, and CD40LT were strikingly lower than those in the supernatants of BALB/c and C57BL/6 B cells (Fig.5C). In addition, 129/SvJ B cell IgE production, unlike that of BALB/c and C57BL/6, was much more independent of cell division, in that the IgE levels in the 129/SvJ B cell supernatants did not increase with decreasing cell concentration as those from the BALB/c and C57BL/6 did. Hasbold *et al* previously reported that B cells must undergo multiple rounds of division before switching to IgE [30]. In an attempt to overcome the defect in IgE production observed in the 129/SvJ B cells, we performed an IL-4 dose response curve. Although IgE levels in BALB/c supernatants increased with increasing concentrations of IL-4, even at 3 fold higher concentrations of IL-4, IgE levels in 129/SvJ B cells were not significantly changed (Fig.5D). After stimulation with IL-4 and CD40LT, mouse B cells class switch from IgM and IgD to IgG1 before switching to

IgE. Similarly to the results we obtained for IgE, IgG1 levels in the 129/SvJ B cell supernatants were also decreased when compared to those from BALB/c (Fig.5B). However, IgG1 levels in the C57BL/6 supernatants were nearly identical to those seen in the 129/SvJ cultures (Fig. 5B), demonstrating the influence of background strain on IgG1 levels.

129/SvJ mice display hyper IgE in vivo

To determine the effect of the 129/SvJ CD23 mutations on IgE regulation *in vivo*, we measured serum IgE levels in BALB/cJ and 129/SvJ mice both before and after immunization with Ag-alum. On day 0, mice were pre-bled by tail vein nick and then injected s.c. with KLH-DNP-alum or alum alone (Fig.6A). Mice were boosted on day 15. Primary and secondary IgE responses were determined at days 9 and 20, respectively. As shown in Fig.6B, baseline IgE levels were substantially higher in 129/SvJ mice than in BALB/cJ mice. Whereas total IgE levels in BALB/cJ mice were less than 500 ng/ml, serum IgE concentrations in 129/SvJ mice ranged from 500 ng/ml to nearly 2 μg/ml. BALB/cJ and 129/SvJ mice injected with KLH-DNP-alum displayed significantly increased total IgE levels at both days 9 and 20 when compared to mice receiving alum alone (Fig.6C and 6D). At both days tested, total IgE levels were significantly elevated in the KLH-DNP-alum immunized 129/SvJ mice as compared to the similarly treated BALB/cJ mice. However, KLH-DNP- specific IgE levels were not statistically different between the 129/SvJ and BALB/cJ strains, suggesting that the hyper IgE phenotype observed in the 129/SvJ strain resulted from increased levels of total IgE (Fig.6E). Next, we examined IgG1 levels in 129/SvJ serum to determine if they were also elevated. Although total IgG1 levels in unimmunized 129/SvJ mice were slightly higher than those in BALB/cJ mice (Avg of 5 mice 148±59 vs 106±53 μgs/ml for Balb vs 129 mice respectively), the difference was not significant. After immunization, total IgG1 levels in BALB/cJ mice were slightly elevated although not statistically different from those in 129/SvJ mice (data not shown). Total IgM levels both before and after immunization were not different between the two strains (187±36 vs 156±64 μg/ml Balb vs 129 mice respectively post immunization).

129/SvJ mice have accelerated clearance of Nippostrongylus brasiliensis

To determine if 129/SvJ mice display hyper IgE in response to parasite infection, we injected 129/SvJ and BALB/cJ mice s.c. with 650 L3 *Nippostrongylus brasiliensis (Nb)*. *Nb* is a helminth that induces a very strong Th2 response, resulting in extremely high IgE levels (μg/ml). Mice were pre-bled on day 0 before injection with *Nb* and then bled on days 15 (peak IgE response) and 43 after infection. Pre-bleed IgE values were significantly higher in the 129/SvJ mice than in the BALB/cJ mice (940±185 vs 275±5 μg/ml, n=7). Total IgE levels at both days 15 (Fig.7A) and 43 (data not shown) were substantially increased in the 129/SvJ mice versus the BALB/cJ mice. At the peak of the response, IgE levels in the 129/SvJ serum ranged from 40 - 90 μg/ml whereas values in the BALB/cJ mice reached approximately 30 μg/ml. The amounts of IgE shown in Fig.7A are the values obtained after background subtraction of the pre-bleed values. Because of the significant increase in IgE levels in the *Nb*-infected 129/SvJ mice versus the *Nb*-infected BALB/cJ mice, we wanted to determine if 129/SvJ mice could clear the infection more rapidly than BALB/cJ mice could. Mice were injected on day 0 with 650 L3. On days 5-9, mice were sacrificed and the small intestines were removed. L5 *Nb* were collected and counted as described in the Materials and Methods. At days 5 and 6, worm burden was reduced in 129/SvJ mice as compared to BALB/cJ mice (data not shown). By day 7, less than 100 worms remained in the intestine of the 129/SvJ mice whereas 150-300 worms were still present in the BALB/cJ (Fig.7B). No worms were recovered from the intestines of the 129/SvJ mice on days 8 or 9 (Fig.7B). BALB/c mice still had substantial worm burden at day 8, but two of the three mice examined on day 9 had cleared the parasites (Fig.7B). Because we had been maintaining our *Nb* cultures by passage through BALB/c mice, we wanted to ensure that the delayed clearance of *Nb* from BALB/c mice was not the effect of an adaptation of *Nb* to these hosts. Therefore, we also compared parasite clearance in 129/SvJ versus C57BL/

6 mice. We measured pre-bleed levels of IgE in the two strains in order to determine if baseline IgE levels were also elevated in 129/SvJ mice versus the C57BL/6 mice. Compared to C57BL/6 mice, 129/SvJ mice had significantly increased baseline levels of IgE and increased clearance of *Nb* (data not shown).

Discussion

In this study, we demonstrate that CD23 mutations are found in mice that have hyper IgE *in vivo*. 129/SvJ, 129P1/ReJ, and NZB mice were found to have five mutations within their CD23 protein. These mutations were associated with reduced B cell CD23 surface expression and consequently, a reduced number of IgE binding sites per cell. In addition, a larger proportion of splenic $B220^+$ B cells were CD23 negative in the 129/SvJ strain than in the BALB/c strain. In agreement with this finding, Kaminski and Stavnezer [16] recently reported a greater proportion of $CD23^-$ $CD19^+$ B cells in the spleens of 129/Sv mice than in C57BL/6 mice. The authors found that this was a result of increased numbers of immature ($CD21^-CD23^-$) and marginal zone ($CD21^{high}CD23^{low}$) B cells in 129/Sv spleens. In contrast, Lewis *et al* [28] reported that while the NZB strain (which has the same CD23 mutations) did have slightly more MZ B cells, the numbers (25% versus 21%) were not significantly increased over those in the C57BL/6 strain. In disagreement with our studies (for the 129/SvJ) and those by Lewis and colleagues (for the NZB), Kaminski and Stavnezer [16] did not find reduced CD23 surface expression on the $CD23^+$ population. This discrepancy may relate to differences in the staining antibodies. We examined CD23 staining using B3B4 and 2H10 (anti-lectin mAbs) as well as rabbit anti-CD23 (polyclonal) while Kaminski and Stavnezer [16] used 2G8 (anti-lectin mAb). In our hands, the 2G8 has a higher non-specific binding even in the presence of FcγR blocking antibodies. This could mask the difference in CD23 expression in $CD23^+$ cells between the strains. Another concern is whether the CD23 mutations present in the 129/SvJ strain alter the antibody epitopes. Indeed one of the anti-lectin monoclonals (2H10) that we examined did not recognize 129/SvJ CD23 (data not shown). Since the differences in CD23 expression observed between the 129/SvJ and BALB/c strains were also seen upon incubation of the respective B cells with IgE and polyclonal anti-CD23 (data not shown), this explanation is unlikely and thus, CD23 expression is indeed reduced in the 129 strain. The IgE data is important for this conclusion. Since the affinity for binding IgE is unchanged, the decrease in anti-IgE staining of the $CD23^+$ peak cannot be the result of the mutations causing less IgE binding. Note that a reproducibly higher number of $B220^+$ cells were $CD23^-$ in the naïve state, although after induction with CD40L and IL-4, virtually all $B220^+$ express at least some CD23 (Fig. 1). Since CD23 message levels are not reduced and the amount of sCD23 detected is lower, the mutant CD23 is most likely being degraded internally.

Sequencing analysis indicated that 5 mutations were present in the 129/SvJ strain. These same mutations were also present in the NZB and 129P1/ReJ mice (Fig 3). The first two mutations (A82T and V87A) are present at the base of the CD23 stalk in the first heptad repeat. The insertion of threonine for alanine at position 82 creates a hydrophilic sidechain which could interrupt CD23's trimeric structure. The other substitution of valine for alanine at position 87 is neutral and therefore unlikely to be disruptive to the CD23 structure. In addition, rat CD23 also contains this same substitution [28]. The third stalk mutation (K131E) replaces lysine with glutamic acid. This is a highly unfavored substitution resulting in the exchange of a basic a.a. for an acidic a.a. and could thus distort the CD23 structure. In addition, this is in close proximity to the region of the CD23 stalk where 19G5 (anti-CD23) binds and thus the K131E mutation could similarly disrupt the CD23 structure. 19G5 binding to the CD23 stalk interferes with the ability of CD23 to bind IgE and destabilizes its trimeric structure, resulting in enhanced CD23 cleavage and IgE synthesis [12]. The S258L mutation within the lectin domain is also unfavorable since it results in a change from a small and polar a.a. to a large and hydrophobic one. Additionally, this change could interfere with the ability of CD23 to bind IgE since

previous studies have demonstrated the necessity of this region for IgE binding [31]. The last mutation (D301N) substitutes an acidic charge for a neutral charge. While this change would not be as unfavorable as the A82T, K131E, or S258L mutations, it is located near two disulphide bridges and thus could be disruptive to their proper formation.

The stalk region has previously been shown to mediate oligomerization of CD23, which is important for high affinity binding to IgE. Despite the presence of three mutations within the 129/SvJ CD23 stalk region (two being unfavored substitutions), there was no difference in the affinities of 129/SvJ or BALB/c CD23 for IgE. Therefore, the mutations are likely interfering with the stability of the protein, thus accounting for the reduced surface levels observed. It should be mentioned that Lewis *et al* [28] found only low affinity binding of NZB CD23 to IgE. However, saturation binding analysis was done by flow cytometry and the accuracy is questionable given the small changes in MFI observed. The reduced sCD23 levels observed in the 129/SvJ strain are a result of lower CD23 surface expression. Although we have not ruled out decreased translation efficiency, the more likely explanation for reduced CD23 surface expression in the 129/SvJ strain is internal degradation of CD23 as a result of the instability caused by the mutations in the stalk

The CD23 mutations in the 129/SvJ and NZB mice are associated with a hyper IgE phenotype *in vivo*. Consistent with our data in the 129/SvJ strain, NZB mice produce significantly more total IgE after immunization with KLH-alum than NZW mice [28]. In addition, several randomly sampled unimmunized NZB mice were also found to have hyper IgE levels. We have demonstrated that both unimmunized and immunized 129/SvJ mice also display hyper IgE. Increased serum IgE in the 129 strain was also reported by Wyczolkowska *et al* [32] in the late 70's although levels were measured by competitive inhibition assay. Yamashita *et al* [17] also reported that the 129 strain had increased baseline levels of IgE although the authors did not examine total or Ag-specific IgE levels after immunization (see below). While there was a trend towards higher IgG1 levels in unimmunized 129/SvJ mice, the difference was not statistically significant. The finding was similar in the NZB strain [28]. There was also no difference in IgM levels between 129/SvJ and BALB/cJ mice either before or after immunization. Therefore, these mice are specifically over-producing IgE. Although total IgE levels in 129/SvJ mice immunized with KLH-DNP-alum were significantly higher (even after subtraction of pre-bleed levels) than those in BALB/cJ mice, antigen-specific IgE levels were similar between the two strains. This suggests that IgE production in the 129/SvJ strain is being driven more strongly by polyclonal activation, than by antigen-mediated activation of B cells. A recent publication by McCoy *et al* [33] described natural IgE production in mice that occurred independently of MHC Class II but required IL-4 and bystander T cell help. It is possible that the hyper IgE levels in the serum of unimmunized 129/SvJ mice results from increased concentrations of IL-4 or CD40 ligand. In addition, 129/SvJ mice could have increased levels of polyclonal IgE secreting plasma cells or plasma cells from these mice could be secreting more IgE on a per cell basis.

High levels of total IgE are associated with protection during parasitic infections. We observed that 129/SvJ mice produce significantly increased levels of total IgE after *Nb* infection compared to BALB/cJ mice. In addition, we observed increased clearance of *Nb* larvae from the intestine of 129/SvJ mice versus both BALB/c and C57BL/6 mice. In separate studies, Nakamura-Uchiyama *et al* [34] found that 129/SvJ mice were naturally resistant to the intestinal nematode *Strongyloides venezuelensis* infection. Because IgE is not required for clearance of *Nb* [35], it is more likely that the increased levels of IgE and the increased clearance of *Nb* from the gut of 129/SvJ versus BALB/cJ mice are a consequence of increased levels of Th2 cytokines in 129/SvJ mice. IL-4 and IL-13 are thought to be critical for clearance of *Nb* [36] and IL-4 is an important IgE switch factor for B cells in mice.

In contrast to the *in vivo* findings, we observed less IgE production in 129/SvJ B cells than in BALB/c or C57BL/6 B cells cultured *in vitro* with IL-4, IL-5 and CD40LT. The 129/SvJ B cells had a boost in early proliferation but by 72 hrs, Balb/B cells had similar cell division numbers. We did consistently observe higher production of IgM than BALB/c B cells. Jongstra-Bilen *et al* [37] have also observed increased proliferation and IgM production *in vitro* in NZB B cells in response to CD40 stimulation in combination with IL-4 or LPS. Corcoran and Metcalf [14] observed significantly reduced expression of the IL-5Rα chain on 129/Sv and 129/Ola B cells which led to defective IL-5 signaling *in vitro*. Culture of the 129/SvJ, BALB/c, and C57BL/6 B cells in the absence of IL-5 did not decrease the amounts of IgE in the BALB/c or C57BL/6 B cells to those levels observed in the 129/SvJ B cells suggesting that the IgE defect in the 129/SvJ mice *in vitro* was not simply a result of decreased IL-5 signaling (data not shown). Addition of increasing concentrations of IL-4 to the cultures did not restore IgE production suggesting that the 129/SvJ B cells are less responsive to IL-4 induced IgE switching *in vitro*. This is important in that B cells from various mouse strains all had similar dose response curves for IgE production with increasing concentrations of IL-4 [38]. Thus, the Th2 or Th1 (or presumably Th17) relatedness of the strain is thought to be independent of B cells. The 129Sv/J and related strains would be the first where B cell switching itself is altered when compared to control (C57 or Balb) in the presence of the same activation signals. The *in vivo* and *in vitro* IgE findings with the 129/SvJ mice are similar to those observed in individuals suffering from Hyper IgE Syndrome (HIES). HIES is an extremely rare primary immunodeficiency characterized by high levels of serum IgE and increased blood eosinophilia. The disease affects multiple organ systems, including the immune system and the skeletal system, and frequently manifests as recurring staphylococcal infections [39]. In addition, PBMCs isolated from the blood of patients with HIES respond similarly to B cells isolated from the spleens of 129/SvJ mice when cultured *in vitro*. PBMCs from HIES donors produced significantly less IgE than PBMCs from either atopic or nonatopic donors when cultured with recombinant human IL-4 (rhIL-4) in the presence or the absence of anti-CD40 [40]. The addition of increasing concentrations of rhIL-4 could not restore IgE production in HIES donor PBMCs. The authors were able to significantly increase IgE levels in rhIL-4 stimulated HIES donor PBMCs by adding ten-fold more anti-CD40 than that added to normal donor PBMCs. However, the levels of IgE in the supernatants of PBMCs cultured from HIES patients were still not as high as those in the supernatants of PBMCs cultured from normal donors. The authors suggested that most blood B cells from HIES patients have already undergone isotype switching *in vivo* and are thus no longer responsive to IL-4 *in vitro* but can synthesize more IgE in response to very high concentrations of a second signal (anti-CD40). This hypothesis is based on studies in which IL-4 was found to be critical for IgE production early in the immune response but played little role after B cells had committed to switching to IgE [41]. King *et al* [42] reported that the amount of IgE secreted per B cell in patients with HIES was significantly reduced but the number of B cells secreting IgE was increased. This finding could explain the results observed with the 129/SvJ mice in which total IgE levels were significantly increased *in vivo* and proliferation was increased *in vitro*.

At this time, we can only correlate the increased IgE levels observed in the 129/SvJ and the NZB mice with the mutations in CD23. However, the finding that two unrelated strains (129 versus NZB) of mice contain exactly the same CD23 mutations as well as hyper IgE levels suggests that the mutations are important with respect to the IgE aberrations found. In addition, F1 mice generated by crossing NZB to NZW mice exhibited hyper IgE levels that were significantly higher than those in NZW mice but not different from those in NZB mice [28], suggesting that the CD23 mutation is dominant and is likely causing the enhancement of IgE. Since there was no detectable difference in the affinity of CD23 for the IgE ligand, the CD23 mutations are likely enhancing IgE production through a loss of cell surface CD23 expression. This supports previous studies using CD23 knockout and CD23Tg mice in which high levels of CD23 were found to be inversely associated with IgE production. Alternatively, since CD23

has other ligands such as CD21 [43] and CD11b [44] mutations could be influencing affinities towards these alternative ligands. This will need to be addressed in future studies.

The 129 substrains are frequently used for gene targeting studies as a result of the availability of embryonic stem cell lines that have been derived from them. Due to the time and cost of breeding, founder animals are frequently incompletely backcrossed away from the 129 background before phenotypic analysis begins. These studies highlight the importance of proper backcrosses and suggest that any knockout mouse created and left on a mixed 129 background will have reduced CD23 and hyper IgE. This can confound experimental interpretation of data, particularly if the gene of interest is thought to influence IgE or CD23 levels. Finally, we would like to propose that the 129/SvJ strain could be beneficial as a mouse model for human hyper-IgE syndrome. No such mouse model has yet been discovered. Study of genetic defects in the 129/SvJ mouse could lead to the identification of potential new targets for therapeutic intervention. Recently, patients with HIES were found to have mutations in their STAT3 binding domain [45]. In addition to STAT3, it is likely that these patients will have other defects that contribute to the immunopathology of the HIES. Thus, the 129/SvJ mouse could be a valuable tool for hyper IgE research.

Acknowledgements

We thank Jerome Schlomer, Witemba Kabange, Yvette Orihuela, Dae-Jong Kang, and Joel Mathews for excellent technical assistance. This work was supported by the U.S. Public Health Service Grant AI18697. J.W.F. was supported in part by the National Institute of Allergy and Infectious Diseases Training Grant T32AI007407.

References

1. Kikutani H, Inui S, Sato R, Barsumian EL, Owaki H, Yamasaki K, Kaisho T, Uchibayashi N, Hardy RR, Hirano T, Tsumasawa S, Sakiyama F, Suemura M, Kishimoto T. Molecular Structure of Human Lymhocyte Receptor for immunoglobulin E. C 1986;47:657–665.
2. Yu LC, Montagnac G, Yang PC, Conrad DH, Benmerah A, Perdue MH. Intestinal epithelial CD23 mediates enhanced antigen transport in allergy: evidence for novel splice forms. Am J Physiol Gastrointest Liver Physiol 2003;285:G223–G234. [PubMed: 12637252]
3. Beavil AJ, Edmeades RL, Gould HJ, Sutton BJ. α-Helical coiled-coil stalks in the low-affinity receptor for IgE (FcεRII/CD23) and related C-type lectins. Proc Natl Acad Sci USA 1992;89:753–757. [PubMed: 1309956]
4. Weskamp G, Ford JW, Sturgill J, Martin S, Docherty AJ, Swendeman S, Broadway N, Hartmann D, Saftig P, Umland S, Sehara-Fujisawa A, Black RA, Ludwig A, Becherer JD, Conrad DH, Blobel CP. ADAM10 is a principal 'sheddase' of the low-affinity immunoglobulin E receptor CD23. Nat Immunol 2006;7:1293–1298. [PubMed: 17072319]
5. Rao M, Lee WT, Conrad DH. Characterization of a monoclonal antibody directed against the murine B lymphocyte receptor for IgE. J Immunol 1987;138:1845–51. [PubMed: 2950171]
6. Sarfati M, Nakajima T, Frost H, Kilchherr E, Delespesse G. Purification and partial biochemical characterization of IgE-binding factors secreted by a human B lymphoblastoid cell line. Immunology 1987;60:539–545. [PubMed: 3495483]
7. Bartlett WC, Kelly AE, Johnson CM, Conrad DH. Analysis of murine soluble Fc epsilon RII sites of cleavage and requirements for dual-affinity interaction with IgE. J Immunol 1995;154:4240–6. [PubMed: 7722284]
8. Yu P, Kosco-Vilbois M, Richards M, Köhler G, Lamers MC, Kohler G. Negative feedback regulation of IgE synthesis by murine CD23. Nature 1994;369:753–756. [PubMed: 8008068]
9. Payet ME, Woodward EC, Conrad DH. Humoral response suppression observed with CD23 transgenics. J Immunol 1999;163:217–223. [PubMed: 10384119]
10. Texido G, Eibel H, Le Gros G, Van der Putten H. Transgene CD23 expression on lymphoid cells modulates IgE and IgG1 responses. J Immunol 1994;153:3028–3042. [PubMed: 8089484]

11. Kilmon MA, Ghirlando R, Strub MP, Beavil RL, Gould HJ, Conrad DH. Regulation of IgE production requires oligomerization of CD23. J Immunol 2001;167:3139–3145. [PubMed: 11544299]
12. Ford JW, Kilmon MA, Haas KM, Shelburne AE, Chan-Li Y, Conrad DH. In vivo murine CD23 destabilization enhances CD23 shedding and IgE synthesis. Cell Immunol 2006;243:107–117. [PubMed: 17324389]
13. Seong E, Saunders TL, Stewart CL, Burmeister M. To knockout in 129 or in C57BL/6: that is the question. Trends Genet 2004;20:59–62. [PubMed: 14746984]
14. Corcoran LM, Metcalf D. IL-5 and Rp105 signaling defects in B cells from commonly used 129 mouse substrains. J Immunol 1999;163:5836–5842. [PubMed: 10570267]
15. McVicar DW, Winkler-Pickett R, Taylor LS, Makrigiannis A, Bennett M, Anderson SK, Ortaldo JR. Aberrant DAP12 signaling in the 129 strain of mice: implications for the analysis of gene-targeted mice. J Immunol 2002;169:1721–1728. [PubMed: 12165492]
16. Kaminski DA, Stavnezer J. Antibody class switching differs among SJL, C57BL/6 and 129 mice. Int Immunol 2007;19:545–556. [PubMed: 17329233]
17. Yamashita Y, Charles N, Furumoto Y, Odom S, Yamashita T, Gilfillan AM, Constant S, Bower MA, Ryan JJ, Rivera J. Cutting edge: genetic variation influences Fc epsilonRI-induced mast cell activation and allergic responses. J Immunol 2007;179:740–743. [PubMed: 17617561]
18. Stief A, Texido G, Sansig G, Eibel H, Le Gros G, Van der Putten H. Mice deficient in CD23 reveal its modulatory role in IgE production but no role in T and B cell development. J Immunol 1994;152:3378–3390. [PubMed: 8144922]
19. Schwartz W, Jiao J, Ford J, Conrad D, Hamel JF, Santanbien P, Bradbury L, Robin T. Application of Chemically-Stable Immunoglobulin-Selective Sorbents: Harvest and Purification of Antibodies with Resolution of Aggregate. BioProcessing Journal 2004;3:53–62.
20. Campbell KA, Lees A, Finkelman FD, Conrad DH. Co-crosslinking FcεRII/CD23 with B cell surface immunoglobulin modulates B cell activation. Eur J Immunol 1992;22:2107–2112. [PubMed: 1386315]
21. DeFranco AL, Raveche ES, Asofsky R, Paul WE. Frequency of B lymphocytes responsive to anti-immunoglobulin. J Exp Med 1982;155:1523–1536. [PubMed: 6802927]
22. McGrew JT, Leiske D, Dell B, Klinke R, Krasts D, Wee SF, Abbott N, Armitage R, Harrington K. Expression of trimeric CD40 ligand in *Pichia pastoris*: Use of a rapid method to detect high-level expressing transformants. Gene 1997;187:193–200. [PubMed: 9099880]
23. Caven TH, Shelburne A, Sato J, Chan-Li Y, Becker S, Conrad DH. IL-21 dependent IgE production in human and mouse in vitro culture systems is cell density and cell division dependent and is augmented by IL-10. Cell Immunol 2005;238:123–134. [PubMed: 16600195]
24. Zhu M, Granillo O, Wen R, Yang K, Dai X, Wang D, Zhang W. Negative regulation of lymphocyte activation by the adaptor protein LAX. J Immunol 2005;174:5612–5619. [PubMed: 15843560]
25. McConahey PJ, Dixon FJ. A method for trace iodination of proteins for immunologic studies. Int Arch Allergy Appl Immunol 1966;29:185–189. [PubMed: 4160044]
26. Kilmon MA, Shelburne AE, Chan-Li Y, Holmes KL, Conrad DH. CD23 trimers are preassociated on the cell surface even in the absence of its ligand, IgE. J Immunol 2004;172:1065–1073. [PubMed: 14707080]
27. Camberis, M.; LeGros, G.; Urban, J, Jr. Animal Model of Nippostrongylus brasiliensis and Heligmosomoides polygyrus. In: Coligan, JE.; Kruisbeek, AM.; Margulies, DH.; Shevach, EM.; Strober, W., editors. Current Protocols in Immunology. John Wiley; New York: 2003.
28. Lewis G, Rapsomaniki E, Bouriez T, Crockford T, Ferry H, Rigby R, Vyse T, Lambe T, Cornall R. Hyper IgE in New Zealand black mice due to a dominant-negative CD23 mutation. Immunogenetics 2004;56:564–571. [PubMed: 15503007]
29. Simpson EM, Linder CC, Sargent EE, Davisson MT, Mobraaten LE, Sharp JJ. Genetic variation among 129 substrains and its importance for targeted mutagenesis in mice. Nat Genet 1997;16:19–27. [PubMed: 9140391]
30. Hasbold J, Lyons AB, Kehry MR, Hodgkin PD. Cell division number regulates IgG1 and IgE switching of B cells following stimulation by CD40 ligand and IL-4. Eur J Immunol 1998;28:1040–1051. [PubMed: 9541600]

31. Bettler B, Texido G, Raggini S, Rüegg D, Hofstetter H. Immunoglobulin E-binding site in Fc_ε receptor (Fc_εRII/CD23) identified by homolog-scanning mutagenesis. J Biol Chem 1992;267:185–191. [PubMed: 1530929]

32. Wyczolkowska J, Michon T, Brzezinska-Blaszczyk E, Maslinski C. The relationship between specific IgE antibody and non-specific IgE in anaphylactic sensitization of mice and rats. Arch Immunol Ther Exp (Warsz) 1982;30:17–23. [PubMed: 7149922]

33. McCoy KD, Harris NL, Diener P, Hatak S, Odermatt B, Hangartner L, Senn BM, Marsland BJ, Geuking MB, Hengartner H, Macpherson AJ, Zinkernagel RM. Natural IgE production in the absence of MHC Class II cognate help. Immunity 2006;24:329–339. [PubMed: 16546101]

34. Nakamura-Uchiyama F, Nagao T, Obara A, Ishiwata K, Nawa Y. Natural resistance of 129/SvJ mice to Strongyloides venezuelensis infection. Parasite Immunol 2001;23:659–663. [PubMed: 11737669]

35. Holland MJ, Harcus YM, Balic A, Maizels RM. Th2 induction by Nippostrongylus secreted antigens in mice deficient in B cells, eosinophils or MHC Class I-related receptors. Immunol Lett 2005;96:93–101. [PubMed: 15585312]

36. Finkelman FD, Shea-Donohue T, Morris SC, Gildea L, Strait R, Madden KB, Schopf L, Urban JF Jr. Interleukin-4- and interleukin-13-mediated host protection against intestinal nematode parasites. Immunol Rev 2004;201:139–155. [PubMed: 15361238]

37. Jongstra-Bilen J, Vukusic B, Boras K, Wither JE. Resting B cells from autoimmune lupus-prone New Zealand Black and (New Zealand Black × New Zealand White)F1 mice are hyper-responsive to T cell-derived stimuli. J Immunol 1997;159:5810–5820. [PubMed: 9550377]

38. Coffman RL, Lebman DA, Rothman P. Mechanism and regulation of immunoglobulin isotype switching. Adv Immunol 1993;54:229–270. [PubMed: 8379463]

39. Grimbacher B, Holland SM, Puck JM. Hyper-IgE syndromes. Immunol Rev 2005;203:244–250. [PubMed: 15661034]

40. Claasen JJ, Levine AD, Schiff SE, Buckley RH. Mononuclear cells from patients with the hyper-IgE syndrome produce little IgE when they are stimulated with recombinant human interleukin-4. J Allergy Clin Immunol 1991;88:713–721. [PubMed: 1720150]

41. Finkelman FD, Holmes J, Urban JF Jr, Paul WE, Katona IM. T help requirements for the generation of an in vivo IgE response: a late acting form of T cell help other than IL-4 is required for IgE but not for IgG1 production. J Immunol 1989;142:403–408. [PubMed: 2521345]

42. King CL, Poindexter RW, Ragunathan J, Fleisher TA, Ottesen EA, Nutman TB. Frequency analysis of IgE-secreting B lymphocytes in persons with normal or elevated serum IgE levels. J Immunol 1991;146:1478–1483. [PubMed: 1899687]

43. Aubry J-P, Pochon S, Graber P, Jansen KU, Bonnefoy J-Y. CD21 is a ligand for CD23 and regulates IgE production. Nature 1992;358:505–507. [PubMed: 1386409]

44. Lecoanet-Henchoz S, Plater-Zyberk C, Graber P, Gretener D, Aubry JP, Conrad DH, Bonnefoy J-Y. Mouse CD23 regulates monocyte activation through an interaction with the adhesion molecule CD11b/CD18. Eur J Immunol 1997;27:2290–2294. [PubMed: 9341771]

45. Minegishi Y, Saito M, Tsuchiya S, Tsuge I, Takada H, Hara T, Kawamura N, Ariga T, Pasic S, Stojkovic O, Metin A, Karasuyama H. Dominant-negative mutations in the DNA-binding domain of STAT3 cause hyper-IgE syndrome. Nature 2007;448:1058–1062. [PubMed: 17676033]

Abbreviations used in this paper

sCD23
: soluble CD23

CD40LT
: CD40 ligand trimer

Nb
: *Nippostrongylus brasiliensis*

KLH
: Keyhole Limpet Hemocyanin

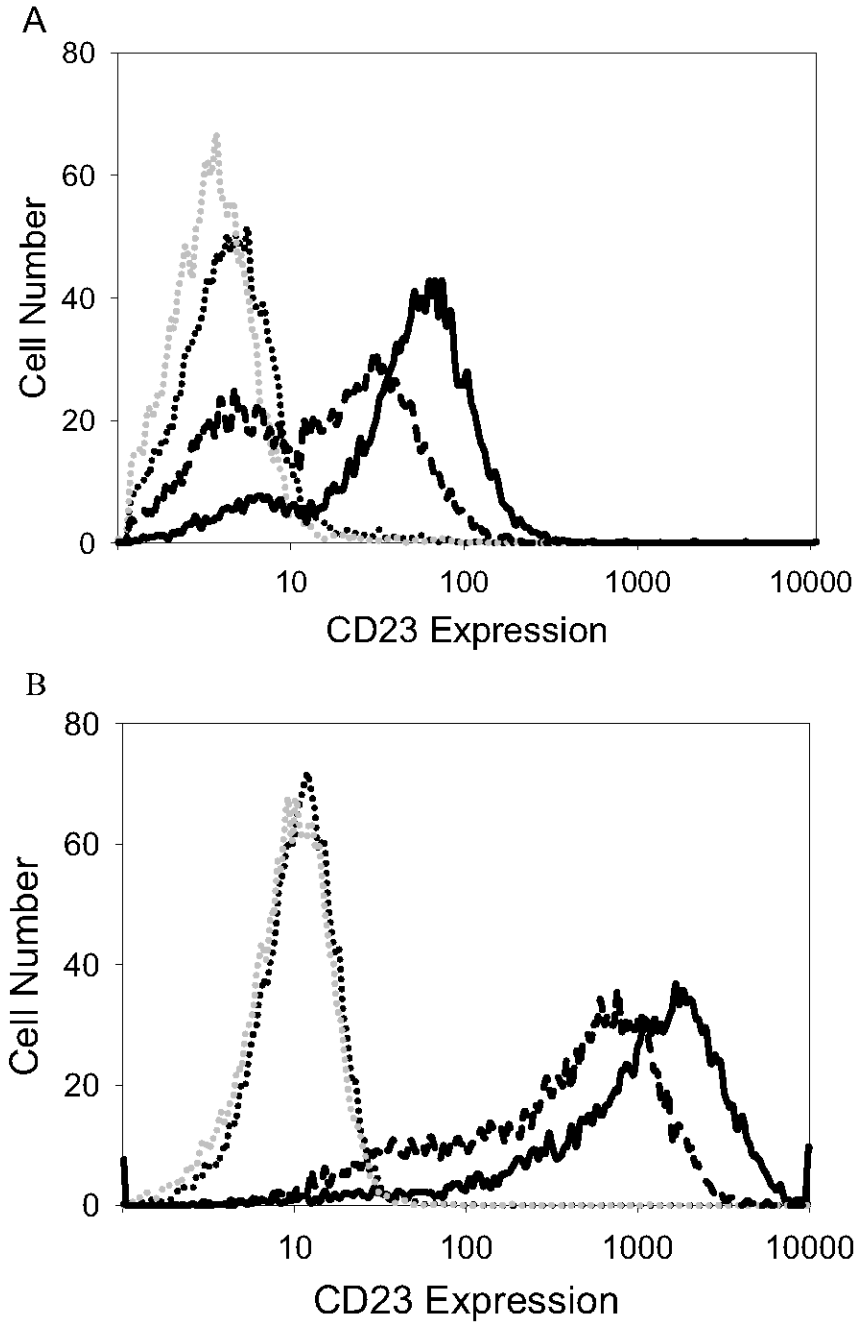

Fig. 1. CD23 surface expression is reduced on 129/SvJ B cells

(A) B cells isolated from the spleens of BALB/c (——) or 129/SvJ (----) mice were stained with B220-APC (B cell marker) in combination with B3B4-FITC (monoclonal anti-CD23). B3B4-FITC histograms are shown gated on the APC+ population. (B) B cells isolated as above were stimulated with IL-4 and CD40LT for 48 hours. B cells were then stained with B220-APC and B3B4-FITC. B3B4-FITC histograms are shown gated on the APC+ population. Controls for Balb/c and 129/SvJ in A and B were stained with B220-APC but left unstained for B3B4-FITC and are shown as dark or gray dotted lines respectively.

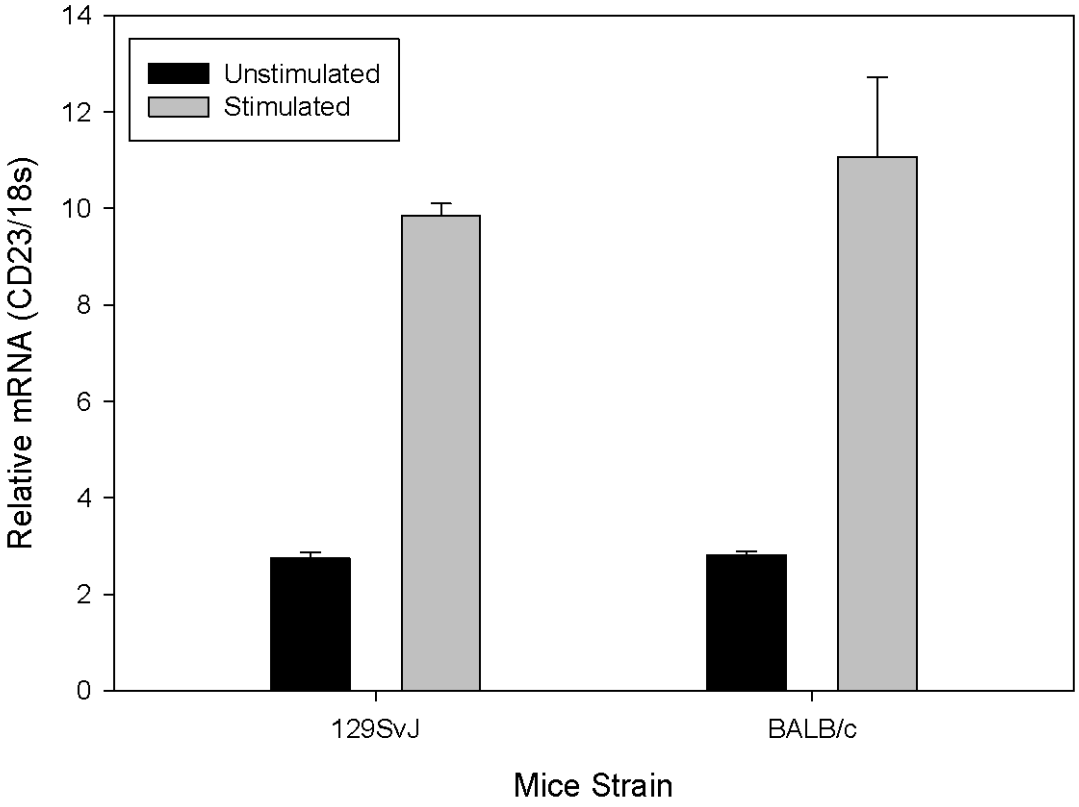

Fig. 2. CD23 message levels are normal in 129/SvJ B cells

B cells isolated from the spleens of BALB/c or 129/SvJ mice were either left untreated or were stimulated with IL-4 and CD40LT for 48 hours. RNA was isolated either immediately (untreated cells) or after the stimulation period, and qPCR was performed using murine CD23 specific primers as described. 18s was amplified as an internal control.

A

```
                1                                                  50
Mouse CD23     (1) MEENEYSGYWEPPRKRCCCARRGTQLMLVGLLSTAMWAGLLALLLLWHWE
 129P1/ReJ     (1) MEENEYSGYWEPPRKRCCCARRGTQLMLVGLLSTAMWAGLLALLLLWHWE
   129Sv/J     (1) MEENEYSGYWEPPRKRCCCARRGTQLMLVGLLSTAMWAGLLALLLLWHWE
       NZB     (1) MEENEYSGYWEPPRKRCCCARRGTQLMLVGLLSTAMWAGLLALLLLWHWE
                   51                                                100
Mouse CD23    (51) TEKNLKQLGDTAIQNVSHVTKDLQKFQSNQLAQKSQVVQMSQNLQELQAE
 129P1/ReJ    (51) TEKNLKQLGDTAIQNVSHVTKDLQKFQSNQLTQKSQAVQMSQNLQELQAE
   129Sv/J    (51) TEKNLKQLGDTAIQNVSHVTKDLQKFQSNQLTQKSQAVQMSQNLQELQAE
       NZB    (51) TEKNLKQLGDTAIQNVSHVTKDLQKFQSNQLTQKSQAVQMSQNLQELQAE
                  101                                               150
Mouse CD23   (101) QKQMKAQDSRLSQNLTGLQEDLRNAQSQNSKLSQNLNRLQDDLVNIKSLG
 129P1/ReJ   (101) QKQMKAQDSRLSQNLTGLQEDLRNAQSQNSELSQNLNRLQDDLVNIKSLG
   129Sv/J   (101) QKQMKAQDSRLSQNLTGLQEDLRNAQSQNSELSQNLNRLQDDLVNIKSLG
       NZB   (101) QKQMKAQDSRLSQNLTGLQEDLRNAQSQNSELSQNLNRLQDDLVNIKSLG
                  151                                               200
Mouse CD23   (151) LNEKRTASDSLEKLQEEVAKLWIEILISKGTACNICPKNWLHFQQKCYYF
 129P1/ReJ   (151) LNEKRTASDSLEKLQEEVAKLWIEILISKGTACNICPKNWLHFQQKCYYF
   129Sv/J   (151) LNEKRTASDSLEKLQEEVAKLWIEILISKGTACNICPKNWLHFQQKCYYF
       NZB   (151) LNEKRTASDSLEKLQEEVAKLWIEILISKGTACNICPKNWLHFQQKCYYF
                  201                                               250
Mouse CD23   (201) GKGSKQWIQARFACSDLQGRLVSIHSQKEQDFLMQHINKKDSWIGLQDLN
 129P1/ReJ   (201) GKGSKQWIQARFACSDLQGRLVSIHSQKEQDFLMQHINKKDSWIGLQDLN
   129Sv/J   (201) GKGSKQWIQARFACSDLQGRLVSIHSQKEQDFLMQHINKKDSWIGLQDLN
       NZB   (201) GKGSKQWIQARFACSDLQGRLVSIHSQKEQDFLMQHINKKDSWIGLQDLN
                  251                                               300
Mouse CD23   (251) MEGEFVWSDGSPVGYSNWNPGEPNNGGQGEDCVMMRGSGQWNDAFCRSYL
 129P1/ReJ   (251) MEGEFVWLDGSPVGYSNWNPGEPNNGGQGEDCVMMRGSGQWNDAFCRSYL
   129Sv/J   (251) MEGEFVWLDGSPVGYSNWNPGEPNNGGQGEDCVMMRGSGQWNDAFCRSYL
       NZB   (251) MEGEFVWLDGSPVGYSNWNPGEPNNGGQGEDCVMMRGSGQWNDAFCRSYL
                  301                           332
Mouse CD23   (301) DAWVCEQLATCEISAPLASVTPTRPTPKSEP-
 129P1/ReJ   (301) NAWVCEQLATCEISAPLASVTPTRPTPKSEP-
   129Sv/J   (301) NAWVCEQLATCEISAPLASVTPTRPTPKSEP-
       NZB   (301) NAWVCEQLATCEISAPLASVTPTRPTPKSEP-
```

B

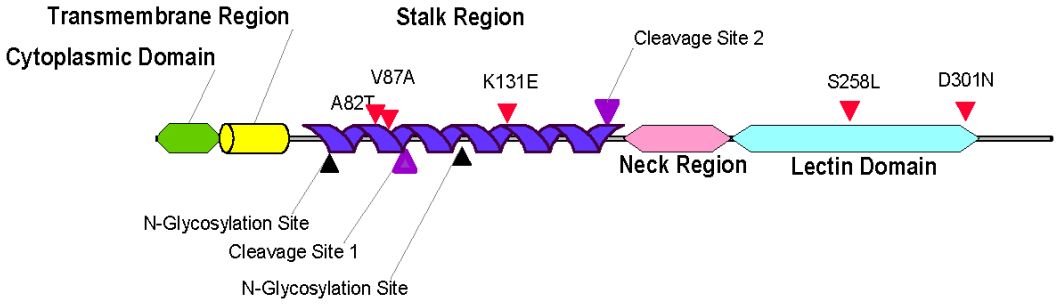

Fig. 3. 129/SvJ, 129P1/ReJ, and NZB CD23 is mutated

(A) CD23 amino acid sequence analysis comparing CD23 from BALB/c, 129/SvJ, 129P1/ReJ, and NZB inbred strains. Five mutations, three in the stalk and two in the lectin domain were observed in the 129/SvJ, 129P1/ReJ, and NZB CD23 as compared to the BALB/c CD23. 129P1/ReJ is a 129 substrain that is related to the 129/SvJ. The NZB strain is unrelated to the 129 strains, but was recently shown to have four of the five mutations (outlined in red boxes) reported here [28]. (B) A schematic diagram of the CD23 protein showing the location of the 5 mutations. See discussion text for details of the mutations and how they may affect the structure of CD23.

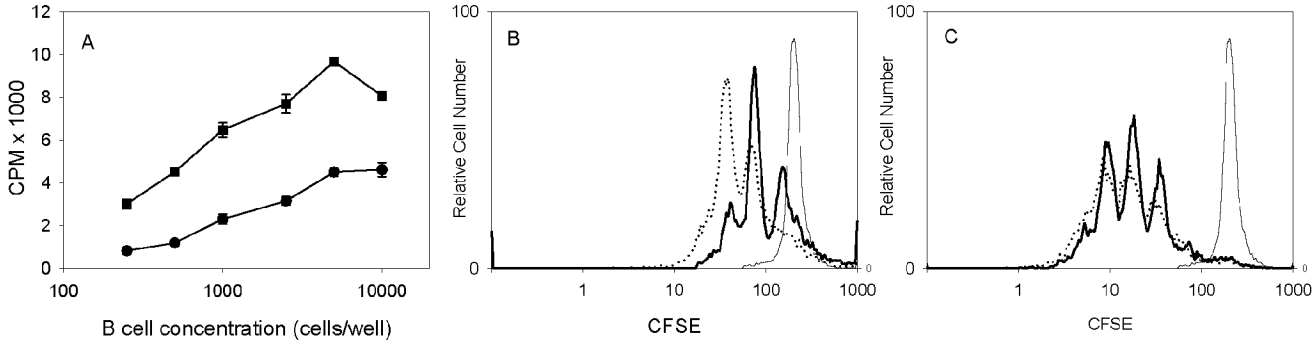

Fig. 4. Transient increase in 129/SvJ B cell proliferation

B cells purified from the spleens of BALB/c and 129/SvJ mice were plated at varying cell concentrations in triplicate and stimulated with IL-4, IL-5, and CD40LT. (A) Proliferation was assessed by measuring [3H]-thymidine incorporation during the last 8 hours of a 72 hour culture period. CFSE labeling after 48 (B) or 72 (C) hrs of culture.

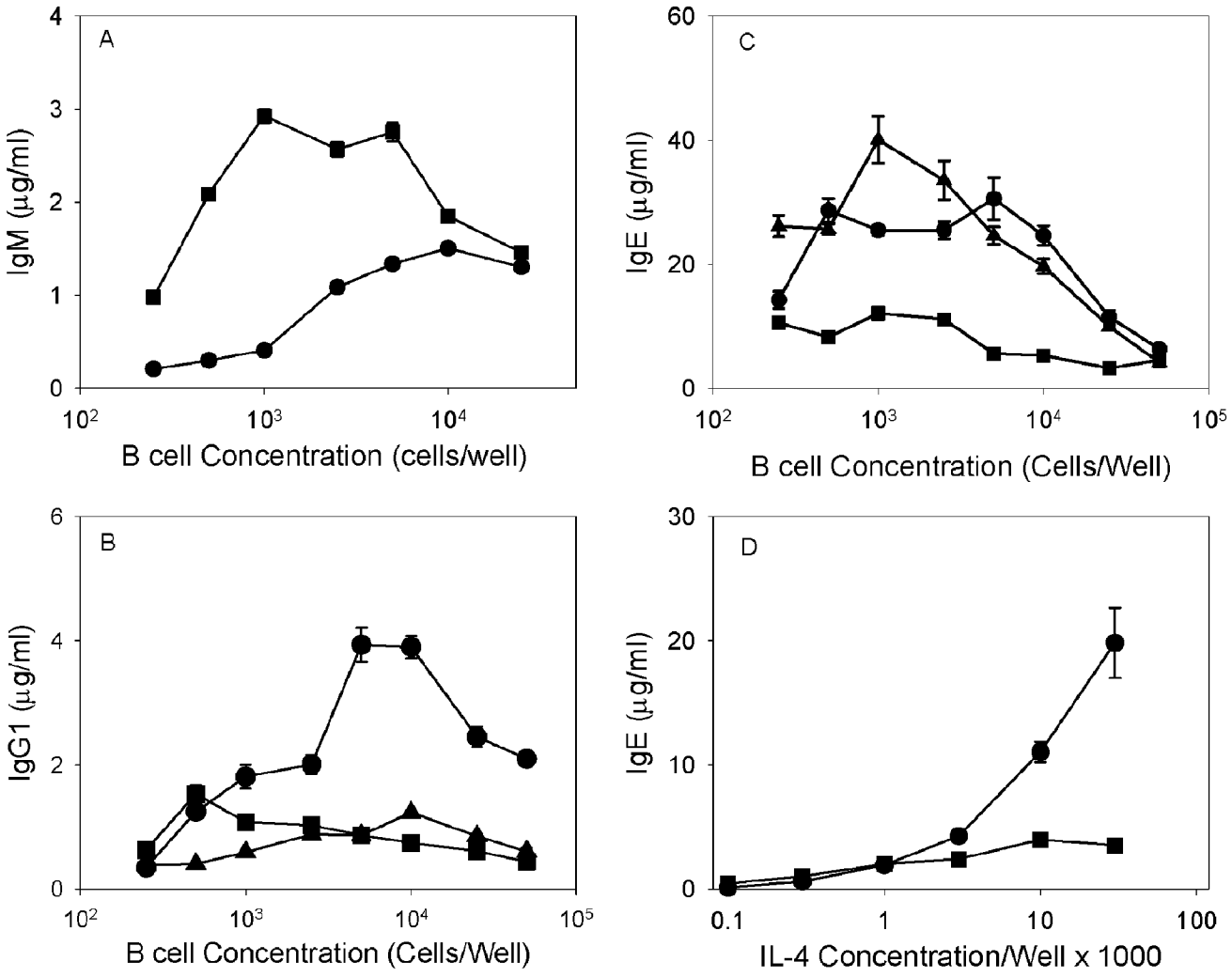

Fig. 5. Decreased IgM and IgE production in B cells from 129/SvJ mice

Purified B cells from BALB/c (●), C57BL/6 (▲), and 129/SvJ (■)mice were plated at varying cell concentrations in triplicate and stimulated with IL-4, IL-5, and CD40LT. Supernatants were harvested on day 9 of culture and (A) IgM or (B) IgG1 or IgE (C) levels were determined by ELISA. (D) 5000 B cells per well from BALB/c or 129/SvJ mice were cultured with IL-5 and CD40LT in the presence of increasing concentrations of IL-4. At day 9 of culture, IgE concentrations in supernatants were assayed by ELISA.

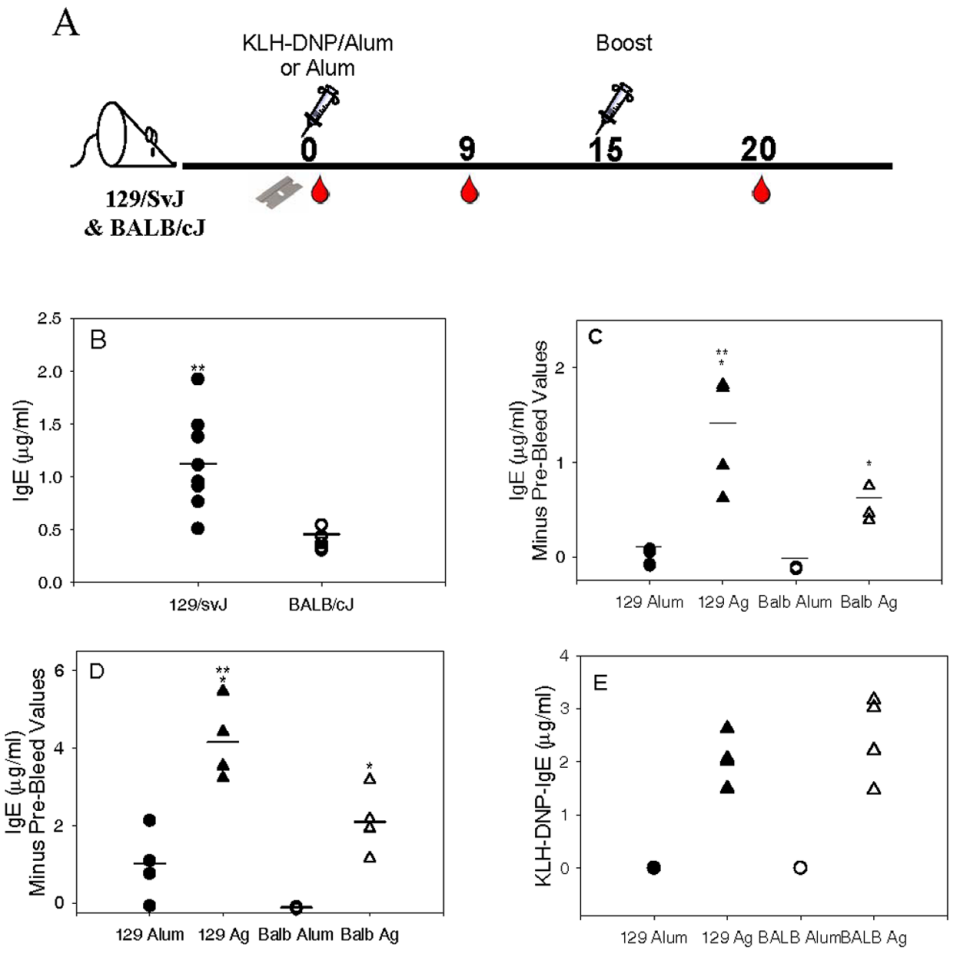

Fig. 6. 129/SvJ mice have hyper IgE *in vivo*

(A) 129/SvJ or BALB/c mice were pre-bled and then injected with KLH-DNP in alum or alum alone. Boosts were performed on day 15. (B) Total IgE levels (assayed by ELISA) in the serum of mice prior to immunization. (C and D) Total IgE levels were determined by ELISA at days (C) 9 and (D) 20 after injection. The values shown were obtained by subtracting the pre-bleed levels (shown in B) from the IgE concentrations measured at days 9 and 20. (E) KLH-DNP-specific IgE concentrations at day 20 were determined by ELISA. Each symbol represents an individual mouse. The average IgE production from each strain is indicated by the black bar. *P* values were <0.05 as determined by Student's *t* test * compares Ag versus Alum within a respective strain (i.e. 129/SvJ Alum vs. 129/SvJ Ag). ** compares 129/SvJ versus BALB/c with respect to similar treatment (i.e. 129/SvJ Ag vs. BALB/cJ Ag).

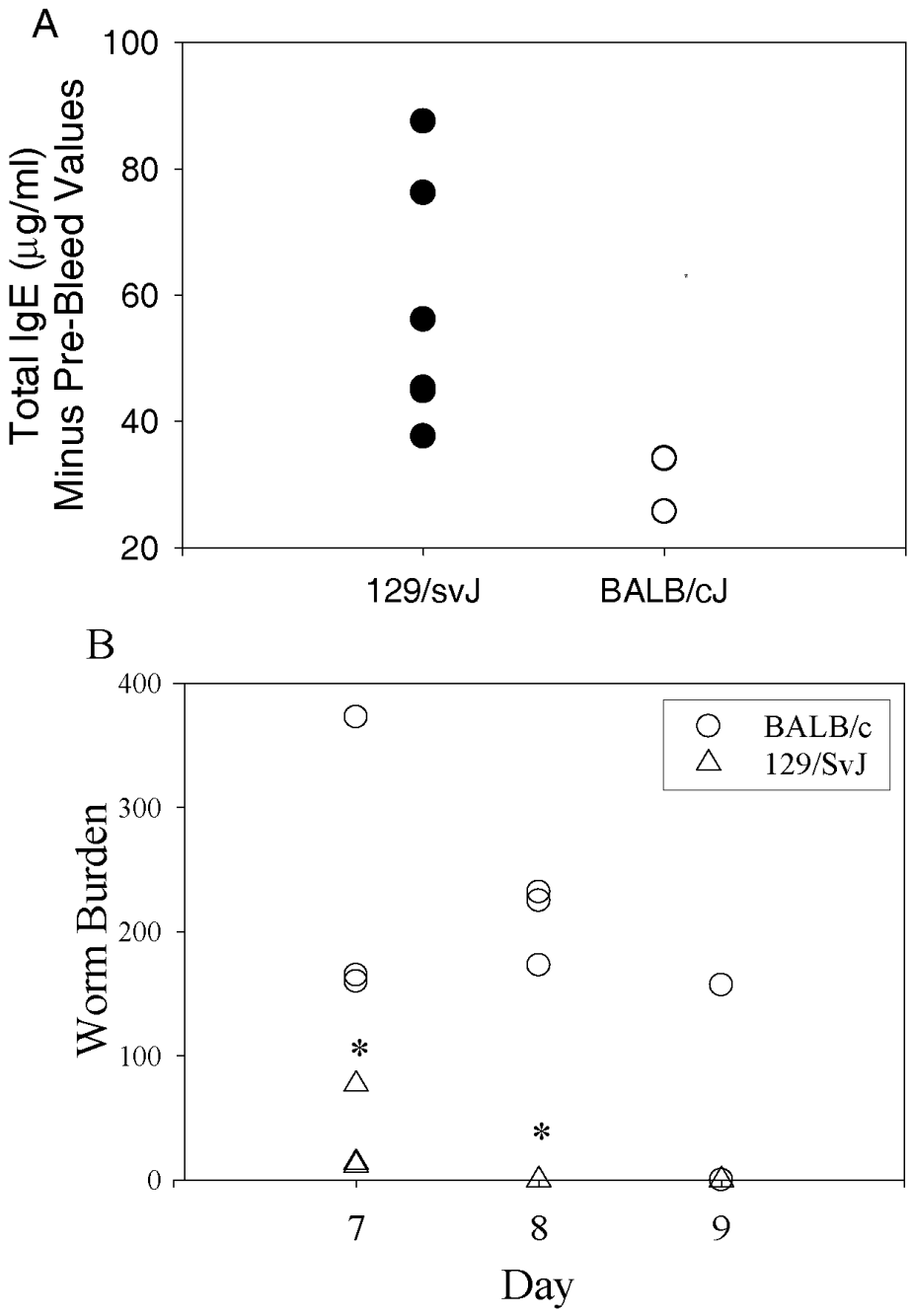

Fig. 7. 129/SvJ mice display hyper IgE and increased clearance of *Nippostrongylus brasiliensis* after helminth infection

BALB/cJ or 129/SvJ mice were injected with 650 L3 *Nippostrongylus brasiliensis*. (A) Total IgE levels at day 15 after infection were determined by ELISA. Values shown are the IgE concentrations remaining after background subtraction of pre-bleed levels. (B) In a separate experiment, 129/SvJ or BALB/c mice were injected as above. On days 5-9 after infection, mice were sacrificed and the intestines were removed. The number of worms recovered on days 7-9 are shown. Each symbol represents an individual mouse. Worm burden from three mice per strain are shown at each day. * indicates a *P* value of <0.05.

Table 1

129/SvJ and BALB/c CD23 bind IgE with a similar affinity but 129/SvJ B cells have a reduced number of IgE binding sites[a].

Mouse strain	Ka Low affinity	Ka High affinity	# of high affinity binding sites	# of low affinity binding sites
BALB/c	$3.82 \times 10^6\ M^{-1}$	$3.46 \times 10^7\ M^{-1}$	144,000	409,000
129/svJ	$2.68 \times 10^6\ M^{-1}$	$3.17 \times 10^7\ M^{-1}$	70,100	218,000

[a] Purified B cells from BALB/c and 129/SvJ mice were stimulated with IL-4 and CD40LT for 48 hours. After harvest, cells were incubated in the presence of increasing concentrations of cold IgE at 37°C. After 1 hour, cell bound counts per minute were determined on duplicate aliquots of cells. Linear regression analysis was performed on Scatchard plots to calculate the affinity constants and number of binding sites. Results shown are the averages of 4 separate experiments. By t-test there was no significant differences ($P<0.1$) between the high or low affinity slopes for the 129 and Balb B cells respectively. However, by t-test, there was a significant difference in the number of high and low affinity binding sites for B cells from the two mouse strains ($P>0.04$).